J. Phys. B: At. Mol. Opt. Phys. **35** (2002) 2195–2203 PII: S0953-4075(02)27971-7

Cross sections of slow electron scattering by cadmium atoms

J E Kontros[1], **L Szótér**[1,2], **I V Chernyshova**[1] **and O B Shpenik**[1]

[1] Institute of Electron Physics, Ukrainian National Academy of Sciences, 21 Universitetska Street, Uzhgorod 88000, Ukraine

[2] Department of Physics, Miskolc University, Miskolc 3515, Hungary

Received 14 August 2001, in final form 26 March 2002
Published 8 May 2002
Online at stacks.iop.org/JPhysB/35/2195

Abstract

The ionization efficiency curve up to 16 eV, the total electron scattering cross section up to 15 eV, the electron excitation cross sections for metastable 5 $^3P_{0,1,2}$ and resonance 5 $^1P_1$ levels up to 11 eV have been measured for cadmium atoms. The energy dependence of the total cross section has revealed two distinctly well resolved resonance features at energies of 0.33 and 3.74 eV, respectively. The total excitation cross sections measured for the 5 $^3P_{0,1,2}$ and 5 $^1P_1$ levels refine the earlier measured optical excitation functions for these levels. These results show the possibility of measuring, in the same experiment, the total cross section of electron scattering by cadmium atoms, the ionization efficiency and the low-lying level excitation function, as well as providing their absolute calibration.

1. Introduction

The relatively heavy cadmium atom with a complex electron structure is a convenient object for experimental studies of a wide class of collision processes. Low-energy electron collisions with cadmium atoms have been studied in a large variety of experimental works (Souter *et al* 1974, Marinkovic *et al* 1991, Buckman and Clark 1994). In spite of this, at present there is a lack of reliable data on the absolute cross sections of elastic electron scattering by cadmium atoms, as well as on the absolute excitation cross sections for the lowest atomic levels (including the metastable ones). This is due to a number of reasons, one of them being the difficulty of calibration of the experimentally measured relative scattering cross section values.

The relative elastic differential and excitation cross sections for 16 levels of the cadmium atom have been studied by Marinkovic *et al* (1991). The energy-loss spectrum at 6.4 eV, measured at an angle of 20°, was found to exhibit contributions of the 5 $^3P_{0,1,2}$, 5 $^1P_1$ and 6 $^3P_1$ levels of the cadmium atom. The triplet 5 $^3P_1$ and 5 $^3P_2$ levels give a noticeable contribution, while there is no contribution from the 5 $^3P_0$ level. Mazing *et al* (1974) studied the excitation of the 5 $^3P_0$ level and found that at 17 eV incident electron energy the absolute value of the

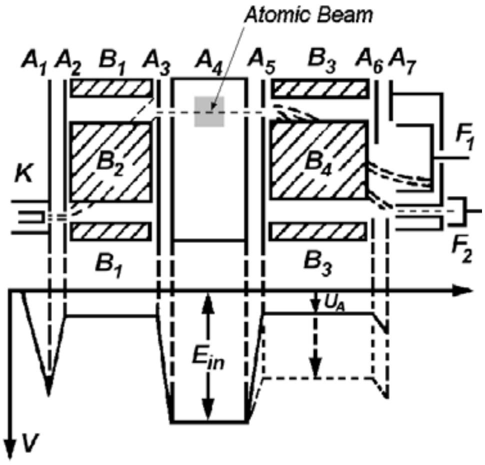

Figure 1. The schematic layout of the HES and potential distribution at its electrodes.

excitation cross section exceeds, by more than one order of magnitude, that for the 5 $^3P_1$ level obtained by the optical method. The discrepancies are probably due to the different cross section calibration techniques used.

In this paper, we report on the possibility of measuring, in the same experiment, the total cross section of electron scattering by cadmium atoms, the ionization efficiency and the low-lying level excitation function at constant scattering geometry and system detection efficiency, as well as performing their absolute calibration. For this purpose the crossed electron and atomic beams technique was used, while a hypocycloidal electron spectrometer (Romanyuk *et al* 1992, Romanyuk and Shpenik 1994) was applied to produce the electron beam (briefly described below). The cadmium atom beam was formed by a compact effusion stainless steel source with a microchannel plate at the exit source. Such a layout of the atomic source in combination with the atomic beam mechanical modulation enabled the background, arising from the electron scattering by residual gases, to be eliminated and a high density value of the atomic beam to be achieved. The mechanical modulation of the beam enables one to shut down the atomic beam using a flag, as described in detail by Mandy *et al* (1995). The residual gas pressure in the collision chamber was 5×10^{-7} Torr.

2. Hypocycloidal electron spectrometer

Our electron spectrometer was comprised of two serially mounted hypocycloidal energy analysers, the first being a primary electron beam monochromator, and the second being an inelastically scattered electron analyser. The schematic layout of the hypocycloidal electron spectrometer (HES) with a typical potential distribution at its electrodes is shown in figure 1.

Electrons were emitted by an oxide cathode K and entered the monochromator (A_1, A_2, A_3, B_1 and B_2 electrodes). In the collision region between the A_4 electrodes, the electron beam was crossed by the atomic beam, then the electrons were directed to the analyser (A_5, A_6, B_3 and B_4 electrodes). At the analyser exit the primary (F_1) and scattered (F_2) electron beam detectors were placed. A non-uniform transverse electric field in the electron monochromator and analyser was created by cylindrical capacitors B_1–B_2 and B_3–B_4, respectively. The electrons were accelerated by the potential difference E_{in} applied between the cathode K and the collision chamber A_4. The electrode A_7 together with a deep Faraday cup F_1 were used for the primary electron beam detection and suppressed the secondary electrons resulting from the electron scattering by the electronic optics surfaces. Inelastically scattered electrons were deflected in the drift area of the analyser, collected through a slit in the electrode A_7 by the second Faraday cup F_2 and measured by a digital nanoammeter. The whole electron spectrometer was placed in an axial uniform magnetic field formed by a pair of Helmholtz rings.

A typical value of the electron energy spread was 0.15 eV (FWHM) in the 0.1–15 eV energy range with a primary electron beam current of $\sim 10^{-7}$ A. Such electron energy spread and beam current values for the primary electron beam passing through the collision chamber were chosen in order to provide identical conditions for carrying out all measurements. The energy scale was calibrated using two methods: through the shift of the current versus voltage characteristic of electron current onto the collector F_1 (see figure 1) and the initial area of the cadmium atom ionization curve. The position of the maximum of the derivative of the initial area of the current versus voltage characteristic was taken as the zero point of the energy scale. The difference in the energy scales determined by the above two methods was ± 0.05 eV.

3. Total scattering cross section

In order to enable the absolute calibration of the scattering cross section to be performed, we first measured the ionization efficiency of the cadmium atom. In this experiment, after monochromatization the electron beam entered the collision chamber and intersected the atomic beam, and the cadmium ions formed in the collision chamber were extracted using a plate with a negative potential and detected by a digital picoammeter. In this case the primary beam passed through the second hypocycloidal analyser without deflection and was collected by the Faraday cup F_1. Great care was taken in selecting the value of the extracting potential at this electrode, mounted normally to the atomic beam direction, because this detects the ions formed in the collision chamber. By carefully choosing this potential with as low a value as possible ($\sim$1.4 V), its influence on the motion of the monochromatized electrons in the collision region was minimized and the total collection of the ions formed was reached.

The well known data of Tawara and Kato (1987) on the absolute σ_i ionization cross sections were ultimately used to calibrate the measured ionization efficiency curve (see figure 2). We only calibrated the ionization curve at a single point (14 eV). The ionization efficiency curve agrees well, in terms of shape, with the ionization efficiency measurements of Hashizume and Wasada (1980), but they carried out no calibration.

When measuring the total electron scattering cross section for cadmium atoms, the scattering geometry remained the same as described above, but all the scattered electrons were collected by the A_4 collision chamber electrodes and detected by a digital nanoammeter. Such an operating mode of the spectrometer was achieved by choosing the potential at the electrodes A_3 and A_5 close to that at the cathode K (see figure 1). These electrodes formed a potential barrier, confining the electrons scattered by the atoms. The total scattering cross section was calibrated according to the formula

$$\sigma_x = \frac{i_x}{I_x}\frac{I_i}{i_i}\sigma_i F^{-1}, \tag{1}$$

where i_x is the scattered electron current when measuring the total scattering cross section (or excitation cross sections) and I_x is the incident electron beam current in the same experiment, i_i is the measured ion current, I_i is the primary electron current value corresponding to the normalization point in the ionization cross section and F is the analyser transmittance. Our analyser is a device that analyses the longitudinal components of the electron velocities.

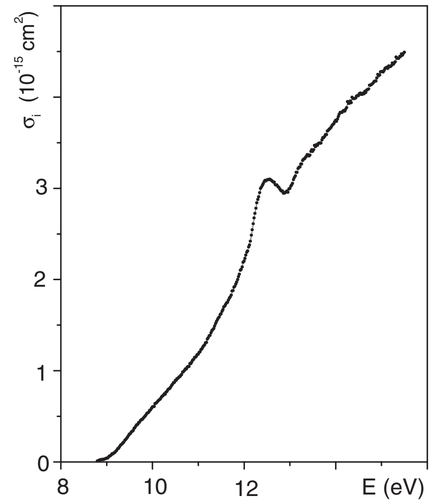

Figure 2. Energy dependence of the ionization cross section for cadmium atoms.

Therefore, all the electrons in the excitation threshold have an energy close to zero, and the analyser detects the total current of inelastically scattered electrons. With increasing incident electron energy and with the angular distribution of the inelastically scattered electrons being taken into account, the electron spectrum produced using the hypocycloidal electron analyser has an energy distribution from the maximum $E_{thr} - E_{exc}$ value to zero. Therefore, the measured curve is not a total level excitation cross section. However, taking into account the presence of a longitudinal magnetic field and using quite 'poor' analyser resolution and the fact that within the limits of scattering angles 0°–30° the differential cross section dominates, the experimentally measured curve reproduces rather well the total excitation cross section. This is supported by the similarity of our measured excitation function for the 5 $^3P_{0,1,2}$ and 5 $^1P_1$ levels with the relevant optical excitation functions (see Shpenik *et al* (1975) and Romanyuk *et al* (1992)).

The measured total cross section is given in table 1. The relative uncertainties in the cross section lie within 3–4% and the absolute uncertainties do not exceed 10%. In figure 3, the energy dependence of the total electron–cadmium atom scattering cross section (curve 1) is shown. When normalizing this curve in accordance with equation (1), the analyser transmittance was not taken into account, since all the scattered electrons were collected by the electrode A_4. Two distinct resonant features are revealed in this curve: a symmetric one at (0.33 ± 0.05) eV, and the second in the vicinity of 4 eV having an asymmetric shape. The energy position of the first feature is in good agreement with the experimental results of Burrow *et al* (1975) and Kazakov (1981). The first feature was extracted from the measured curve by subtracting the linearly interpolated background below the feature and is shown in inset (a) in figure 3.

The second feature was extracted from the measured curve by subtracting the polynomial interpolated background and is presented in inset (b) of figure 3. The resulting feature at $E_p = (3.74 \pm 0.05)$ eV has the Fano–Cooper shape (see, for example, Massey (1976)) and its energy position and width were determined by the technique used in our earlier paper (Shpenik *et al* 1975). We have found the value $\Gamma = (0.52 \pm 0.05)$ eV and the Fano asymmetry parameter $q = 1.67$. The maximum of this resonance shape is observed at 4.1 eV and agrees well with the classification of Buckman and Clark (1994). Note that the change of shape of the

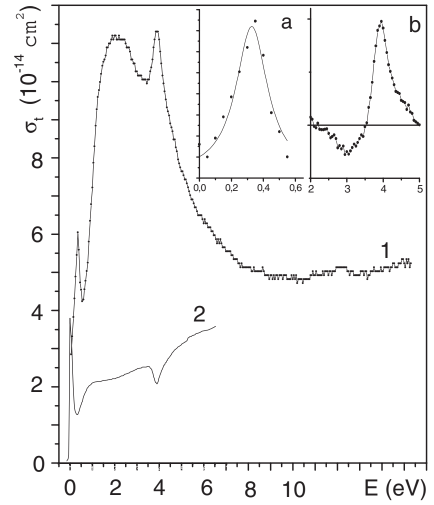

Figure 3. Energy dependence of the total electron–cadmium atom scattering cross section. Curve 1—our measurement for the total cross section, curve 2—the transmission experiment of Burrow *et al* (1976) in relative units; inset (a) represents the behaviour of the $5s^25p$ ^2P resonance fitted by the Lorentz distribution and inset (b) represents the extracted common behaviour of the resonance feature near the $5\ ^3P_{0,1,2}$ levels of cadmium.

$5s5p^2$ Cd^- resonance at different scattering angles was observed by Sullivan *et al* (1999) and Buckman *et al* (1999) who found the decay of this resonance to contribute essentially to the elastic scattering channel. The resonance of such type is known to be located slightly above its parent level. In this energy range the $5\ ^3P_0$ (3.734 eV), $5\ ^3P_1$ (3.801 eV) and $5\ ^3P_2$ (3.946 eV) cadmium atom levels with the 5s5p outer-shell configuration are located (Marinkovic *et al* 1991). Hence the $5s5p^2$ $^2P_{1/2}$ state of the cadmium negative ion, revealed in our curve at 3.74 eV, can decay to the $5\ ^3P_0$ level as well as contribute to the elastic scattering channel. Unfortunately, we have found no resonance feature near the $5\ ^1P_1$ cadmium level, though Burrow *et al* (1976) observed it as a shoulder at 5.4 eV.

4. Total excitation cross section of the $5\ ^3P_{0,1,2}$ levels

In the case of measuring the total excitation function the electron beam after monochromatization by the first energy analyser entered the collision chamber, where it intersected the atomic beam. Then the scattered electrons were analysed by the second energy analyser, where they were deflected in the crossed electric and magnetic fields and collected by the second Faraday cup F_2. The potentials at the electrodes A_5, A_6 and A_7 of the second energy analyser were chosen to provide the detection of the scattered electrons with energy losses equal to the excitation energy of the metastable $5\ ^3P_{0,1,2}$ levels.

The measured excitation cross section of the cadmium atom $5\ ^3P_{0,1,2}$ levels is shown in figure 4. The cross section was normalized using equation (1), as shown above. The analyser transmittance was 0.85. Besides the main maximum at 4.2 eV the measured curve reveals a feature near the $^1P_1$ level threshold and a structure in the 6–11 eV energy range. Note that after calibration the total cross section for the $5\ ^3P_{0,1,2}$ levels excitation is 1.05×10^{-15} cm^2 at the maximum and 3×10^{-16} cm^2 at 10 eV. The latter value agrees fairly well with the results of Mazing *et al* (1974), where the $5\ ^3P_0$ level excitation cross section value of 1.8×10^{-16} cm^2 was obtained at 17 eV energy.

Table 1. Total electron scattering cross sections for the cadmium atom.

E (eV)	σ_{tot} (10^{-14} cm^2)	E (eV)	σ_{tot} (10^{-14} cm^2)	E (eV)	σ_{tot} (10^{-14} cm^2)	E (eV)	σ_{tot} (10^{-14} cm^2)
0.05	2.85	2.65	10.89	5.25	7.33	7.85	5.13
0.1	3.32	2.7	10.78	5.3	7.23	7.9	5.13
0.15	3.82	2.75	10.58	5.35	7.12	7.95	5.13
0.2	4.31	2.8	10.58	5.4	7.02	8	5.13
0.25	4.89	2.85	10.47	5.45	6.91	8.05	5.13
0.3	5.45	2.9	10.47	5.5	6.91	8.1	5.13
0.35	6.04	2.95	10.26	5.55	6.81	8.15	5.03
0.4	5.59	3	10.26	5.6	6.70	8.2	5.03
0.45	4.73	3.05	10.16	5.65	6.70	8.25	5.13
0.5	4.54	3.1	10.16	5.7	6.59	8.3	5.03
0.55	4.24	3.15	10.16	5.75	6.49	8.35	5.03
0.6	4.28	3.2	10.16	5.8	6.49	8.4	5.03
0.65	4.55	3.25	10.05	5.85	6.49	8.45	5.03
0.7	4.77	3.3	10.05	5.9	6.49	8.5	5.03
0.75	5.03	3.35	10.05	5.95	6.39	8.55	5.03
0.8	5.25	3.4	10.05	6	6.28	8.6	5.03
0.85	5.80	3.45	9.95	6.05	6.39	8.65	5.13
0.9	6.34	3.5	10.05	6.1	6.28	8.7	5.03
0.95	6.78	3.55	10.05	6.15	6.28	8.75	4.92
1	7.22	3.6	10.26	6.2	6.18	8.8	4.92
1.05	7.87	3.65	10.37	6.25	6.18	8.85	4.92
1.1	8.30	3.7	10.58	6.3	6.18	8.9	4.92
1.15	8.84	3.75	10.89	6.35	6.07	8.95	4.82
1.2	9.27	3.8	11.10	6.4	6.07	9	4.92
1.25	9.59	3.85	11.31	6.45	5.97	9.05	4.92
1.3	9.77	3.9	11.31	6.5	5.97	9.1	4.82
1.35	9.99	3.95	11.31	6.55	5.87	9.15	4.92
1.4	10.20	4	11.10	6.6	5.76	9.2	4.82
1.45	10.41	4.05	10.79	6.65	5.86	9.25	4.92
1.5	10.52	4.1	10.47	6.7	5.76	9.3	4.92
1.55	10.58	4.15	10.16	6.75	5.86	9.35	4.82
1.6	10.68	4.2	9.95	6.8	5.76	9.4	4.92
1.65	10.89	4.25	9.74	6.85	5.65	9.45	4.92
1.7	10.89	4.3	9.53	6.9	5.65	9.5	4.92
1.75	10.99	4.35	9.32	6.95	5.65	9.55	4.82
1.8	10.99	4.4	9.21	7	5.55	9.6	4.92
1.85	11.10	4.45	9.11	7.05	5.55	9.65	4.92
1.9	11.20	4.5	8.90	7.1	5.55	9.7	4.92
1.95	11.10	4.55	8.79	7.15	5.55	9.75	4.82
2	11.20	4.6	8.69	7.2	5.55	9.8	4.82
2.05	11.20	4.65	8.48	7.25	5.44	9.85	4.82
2.1	11.10	4.7	8.48	7.3	5.44	9.9	4.82
2.15	11.10	4.75	8.27	7.35	5.34	9.95	4.92
2.2	11.20	4.8	8.17	7.4	5.34	10	4.82
2.25	11.10	4.85	7.96	7.45	5.34	10.05	4.92
2.3	11.10	4.9	7.85	7.5	5.34	10.1	4.82
2.35	11.10	4.95	7.75	7.55	5.23	10.15	4.92
2.4	11.10	5	7.64	7.6	5.23	10.2	4.71
2.45	11.10	5.05	7.64	7.65	5.13	10.25	4.82
2.5	10.99	5.1	7.54	7.7	5.24	10.3	4.82
2.55	10.89	5.15	7.43	7.75	5.13	10.35	4.82
2.6	10.89	5.2	7.43	7.8	5.13	10.4	4.82

Table 1. (Continued.)

E (eV)	σ_{tot} (10^{-14} cm^2)	E (eV)	σ_{tot} (10^{-14} cm^2)	E (eV)	σ_{tot} (10^{-14} cm^2)	E (eV)	σ_{tot} (10^{-14} cm^2)
10.45	4.71	11.7	5.03	12.95	4.92	14.2	5.13
10.5	4.82	11.75	4.92	13	4.92	14.25	5.13
10.55	4.82	11.8	5.03	13.05	5.03	14.3	5.13
10.6	4.82	11.85	5.03	13.1	5.03	14.35	5.03
10.65	4.82	11.9	5.03	13.15	5.03	14.4	5.13
10.7	4.82	11.95	5.13	13.2	4.92	14.45	5.13
10.75	4.82	12	5.13	13.25	5.03	14.5	5.24
10.8	4.92	12.05	5.13	13.3	5.03	14.55	5.24
10.85	4.92	12.1	5.13	13.35	4.82	14.6	5.13
10.9	5.03	12.15	5.13	13.4	4.92	14.65	5.13
10.95	4.92	12.2	5.13	13.45	4.92	14.7	5.13
11	4.92	12.25	5.13	13.5	5.03	14.75	5.24
11.05	5.03	12.3	5.13	13.55	5.03	14.8	5.24
11.1	4.92	12.35	5.13	13.6	5.03	14.85	5.24
11.15	4.92	12.4	5.13	13.65	5.13	14.9	5.34
11.2	4.92	12.45	5.03	13.7	5.03	14.95	5.34
11.25	4.92	12.5	5.03	13.75	5.03	15	5.24
11.3	4.92	12.55	4.92	13.8	5.03	15.05	5.13
11.35	5.03	12.6	5.03	13.85	5.03	15.1	5.34
11.4	4.92	12.65	5.03	13.9	5.03	15.15	5.24
11.45	5.03	12.7	5.03	13.95	5.13	15.2	5.34
11.5	5.03	12.75	4.92	14	5.03	15.25	5.13
11.55	5.03	12.8	4.92	14.05	5.03	15.3	5.24
11.6	4.92	12.85	4.92	14.1	5.13		
11.65	5.03	12.9	4.92	14.15	5.13		

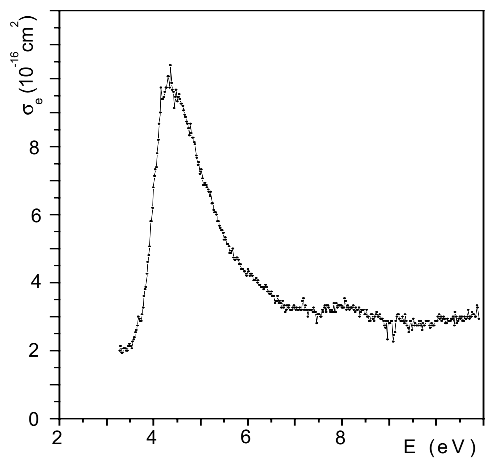

Figure 4. Total averaged excitation cross section for the cadmium atom 5 $^3P_{0,1,2}$ levels.

5. 5 $^1P_1$ level excitation

When measuring the excitation cross section of the $^1P_1$ level the technique was similar to that described in the previous section. The potentials at the electrodes A_5, A_6 and A_7 were chosen

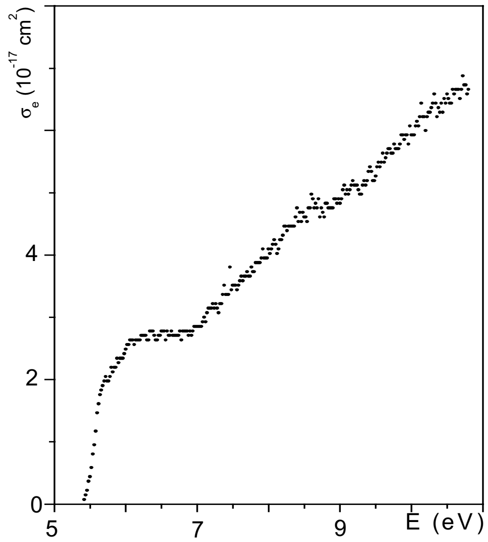

Figure 5. Excitation cross section for the cadmium atom 5 $^1P_1$ level.

to detect the scattered electrons, having lost energy equal to the energy of the cadmium $^1P_1$ level excitation. The analyser transmittance, as mentioned above, was 0.85.

The measured and normalized excitation cross section of the cadmium atom resonance $^1P_1$ level is shown in figure 5. It reveals a broad feature near 6.8 eV probably related to the $4d^{10}5s5p^2$ negative-ion state (see Buckman and Clark (1994)) whose parent level is the 6 $^3P_1$ of the neutral atom and is resolved in the optical excitation function for the 5 $^1P^1$ level from Shpenik *et al* (1973). Another feature at 8.4 eV correlates well with the maxima in the optical excitation function for the 7 $^3S_1$ level (Shpenik *et al* 1973). The absolute excitation cross section for the $^1P_1$ level, measured by an optical technique, is 1.1×10^{-16} cm^2 at 14 eV. This agrees with the results of our measurements.

6. Conclusions

HES together with the effusion microchannel source of metal atoms enabled the absolute cross sections of different processes to be measured in the same experiment as well as the data on the mechanisms of atomic level population to be investigated. The advantages of HES are especially important in the range of very small scattering energies, where the essential role is played by the short-lived negative-ion states.

The obtained absolute cross sections of electron scattering by cadmium atoms refine and complement the available atomic data, allowing the relative role of the short-lived negative-ion states to be evaluated. Our measurements performed for cadmium atoms have confirmed, once again, the presence of a resonance feature in the elastic channel.

Acknowledgment

The research described in this paper was performed, in part, under Award no UP2-2118 of the CRDF.

References

Buckman S J and Clark C W 1994 *Rev. Mod. Phys.* **66** 519
Buckman S J *et al* 1999 *Aust. J. Phys.* **52** 473
Burrow P D, Michejda J A and Comer J 1976 *J. Phys. B: At. Mol. Phys.* **9** 3225
Hashizume A and Wasada N 1980 *J. Phys. B: At. Mol. Phys.* **13** 4865
Kazakov S M 1981 *Pis. JETP* **7** 900 (in Russian)
Mandy I A, Romanyuk M I, Papp F F and Shpenik O B 1995 *Instrum. Exp. Techniques* **38** 368 (in Russian)
Marinkovic B, Pejcev V, Filipovic D and Vuskovic L 1991 *J. Phys. B: At. Mol. Opt. Phys.* **24** 1817
Massey H 1976 *Negative Ions* (Cambridge: Cambridge University Press) p 751
Mazing M A, Rakhovskii V I, Stotskii G I and Shustrikov V M 1974 *Opt. Spectrosc.* **37** 464
Romanyuk M I and Shpenik O B 1994 *Meas. Sci. Technol.* **5** 912
Romanyuk M I, Shpenik O B, Papp F F, Cheryshova I V, Mandy J A, Kelemen V I, Sabad O P and Remeta E Yu 1992 *Ukr. Phys. J.* **37** 1639
Shpenik O B, Souter V V, Zavilopulo A N, Zapesochny I P and Kontrosh J E 1975 *JETP* **69** 48 (in Russian)
Shpenik O B, Zapesochny I P, Souter V V, Kontrosh E A and Zavilopulo A N 1973 *JETP* **65** 1797 (in Russian)
Souter V V, Zapesochny I P and Shpenik O B 1974 *Opt. Spectrosc.* **36** 826 (in Russian)
Sullivan J P, Buckman S J, Newman D S, McEachran R P, Burrow P D and Bartschat K 1999 *21st Int. Conf. on Physics of Electronic and Atomic Collisions (Sendai, Japan)* vol 1 p 264 (Abstracts of Contributed Papers)
Tawara H and Kato K 1987 *At. Data Nucl. Data Tables* **36** 312